THE JOURNAL OF BIOLOGICAL CHEMISTRY VOL. 286, NO. 20, pp. 17631–17639, May 20, 2011

Adenovirus E3-19K Proteins of Different Serotypes and Subgroups Have Similar, Yet Distinct, Immunomodulatory Functions toward Major Histocompatibility Class I Molecules*

Received for publication, December 13, 2010, and in revised form, March 13, 2011 Published, JBC Papers in Press, March 25, 2011, DOI 10.1074/jbc.M110.212050

Jie Fu, Lenong Li, and Marlene Bouvier[1]

From the Department of Microbiology and Immunology, University of Illinois, College of Medicine, Chicago, Illinois 60612

Our understanding of the mechanism by which the E3-19K protein from adenovirus (Ad) targets major histocompatibility complex (MHC) class I molecules for retention in the endoplasmic reticulum is derived largely from studies of Ad serotype 2 (subgroup C). It is not well understood to what extent observations on the Ad2 E3-19K/MHC I association can be generalized to E3-19K proteins of other serotypes and subgroups. The low levels of amino acid sequence homology between E3-19K proteins suggest that these proteins are likely to manifest distinct MHC I binding properties. This information is important as the E3-19K/MHC I interaction is thought to play a critical role in enabling Ads to cause persistent infections. Here, we characterized interaction between E3-19K proteins of serotypes 7 and 35 (subgroup B), 5 (subgroup C), 37 (subgroup D), and 4 (subgroup E) and a panel of HLA-A, -B, and -C molecules using native gel, surface plasmon resonance (SPR), and flow cytometry. Results show that all E3-19K proteins exhibited allele specificity toward HLA-A and -B molecules; this was less evident for Ad37 E3-19K. The allele specificity for HLA-A molecules was remarkably similar for different serotypes of subgroup B as well as subgroup C. Interestingly, all E3-19K proteins characterized also exhibited MHC I locus specificity. Importantly, we show that Lys^{91} in the conserved region of Ad2 E3-19K targets the C terminus of the α2-helix (MHC residue 177) on MHC class I molecules. From our data, we propose a model of interaction between E3-19K and MHC class I molecules.

Ads[2] are widespread in the human population, with at least 51 human serotypes (Ad1 to Ad51) known that are classified into six subgroups (A–F) (1, 2). Following primary infection of the respiratory tract, Ads of subgroup C (the most commonly studied subgroup) can be recovered from stool for months, and even years, after the virus is no longer detected in nasopharyngeal specimens (3, 4). It is believed that this is a manifestation of the ability of Ads to counteract host antiviral immune responses and establish persistent infections. Diseases caused by Ad infections are generally mild except in immunosuppressed individuals, such as AIDS patients and transplant recipients, in which case Ad infections can be fatal (5–8).

It was first shown that Ad2 could drastically decrease the expression of MHC class I molecules on Ad2-infected cells (9–11). The E3-19K protein of Ad2 was found to be specifically responsible for this effect (11). It is now understood that E3-19K binds directly to and retains MHC class I molecules in the ER. Consequently, E3-19K down-regulates MHC class I molecules on Ad-infected cells and protects cells from recognition and lysis by allospecific CTLs (9–17). E3-19K-mediated suppressing effects on CTL activity were shown in Ad-infected human and mouse cells (15, 16, 18). Moreover, *in vivo* data support a role for E3-19K in Ad infections (19); lungs of cotton rats infected with a mutant Ad containing a deletion in the gene encoding E3-19K caused a more severe immunopathology than lungs infected with wild-type Ad. It was suggested that the absence of E3-19K in the mutant virus activated CTLs as part of the inflammatory response to the infection (19). Thus, there is convincing evidence from *in vitro* and *in vivo* studies that E3-19K, through its association with MHC class I molecules, facilitates the undetected replication of the virus in infected host cells. This is thought to contribute to the ability of Ads to establish and maintain persistence (19–21).

E3-19K is a type I transmembrane glycoprotein that includes an N-terminal ER lumenal domain and a short C-terminal cytosolic tail. The ER lumenal domain of E3-19K binds with high affinity to the ER lumenal domain of MHC class I molecules (12, 22–26), and the dilysine motif in the cytosolic tail of E3-19K provides the signal for localization in the ER (12, 27, 28). The ER lumenal domain of E3-19K has been subdivided into three regions with loosely defined boundaries (26, 29) as follows: 1) residues 1 to ~78/81 are rather variable between E3-19K proteins of different subgroups; 2) residues ~79/82 to 98 are rather conserved between E3-19K proteins of different subgroups; and 3) residues 99 to 107 link the ER lumenal domain to the transmembrane domain. To date, we have a limited understanding of how the variable and conserved regions of E3-19K are involved in targeting MHC class I molecules. Similarly, we have a weak understanding of how the low levels of sequence homology (as low as ~34%) between E3-19K proteins of different serotypes and subgroups affect their immunomodulatory function. It is reasonable to assume that such significant differences in sequences will translate into differential MHC I binding properties. Consistent with this view, we showed previously

* This work was supported, in whole or in part, by National Institutes of Health Grant AI045070 from NIAID. This work was also supported by University of Illinois at Chicago, Center for Clinical and Translational Science Award UL1RR029879 from the NCRR.

[1] To whom correspondence should be addressed: Dept. of Microbiology and Immunology M/C 790, University of Illinois College of Medicine, 835 S. Wolcott Ave., Chicago, IL 60612. Tel.: 312-355-0664; Fax: 312-996-6415; E-mail: mbouvier@uic.edu.

[2] The abbreviations used are: Ad, adenovirus; ER, endoplasmic reticulum; CTL, cytotoxic T lymphocyte; SPR, surface plasmon resonance; β_2m, β_2-microglobulin; NK, natural killer.

that Ad2 E3-19K associates with MHC class I molecules in an allele- and locus-specific manner (30, 31). It was also reported that Ad2 E3-19K co-immunoprecipitated more readily with HLA-A2 than HLA-B7 (32). Furthermore, it was shown previously that Ad2 and Ad19a E3-19K proteins of subgroups C and D, respectively, differ in their capacity to inhibit the trafficking of MHC class I molecules to the cell surface (12). This kind of information on the MHC I binding function of E3-19K proteins of different Ad serotypes and subgroups is critical not only for our understanding of the structure/function relationship of E3-19K but also because it is thought that the ability of a particular Ad serotype to replicate and establish persistent infection in host cells may depend on the avidity of its E3-19K protein for the HLA molecules present in the infected individual (21, 33). There is therefore an epidemiological component to our understanding of Ad pathogenesis that can be probed from a systematic study of E3-19K function across Ad serotypes and subgroups.

In this study, we carried out a systematic analysis of interaction between E3-19K proteins of Ad serotypes 7 and 35 (subgroup B), 5 (subgroup C), 37 (subgroup D), and 4 (subgroup E) and HLA-A (A*0301, A*1101, A*3101, A*3301, and Aw*6801), HLA-B (B*0702 and B*0801), and HLA-C (Cw*0304 and Cw*0401) molecules using site-directed mutagenesis, native gel, SPR, and flow cytometry. A molecular and cellular characterization of E3-19K proteins across serotypes and subgroups will provide a more in-depth understanding of its immunomodulatory function and will also generate knowledge relevant for advances in Ad pathogenesis.

EXPERIMENTAL PROCEDURES

Cell Lines and mAbs—The human HLA-A and -B negative B-cell line C1R stably expressing HLA-A*1101 (A11/C1R; a gift from Dr. R. Gavioli, University of Ferrara, Ferrara, Italy) and HLA-A*3101 (A31/C1R (31)) were maintained in RPMI 1640 medium (Invitrogen) containing 200 μg/ml hygromycin B (Mediatech) and 300 μg/ml G418 (Calbiochem). W6/32 (Abcam), anti-HLA-A11 (One Lambda), and anti-HLA-A31 (One Lambda) were used as primary Abs, FITC-conjugated rat anti-mouse IgG (eBioscience) and FITC-conjugated goat anti-mouse IgM (Jackson ImmunoResearch) were used as secondary Abs in flow cytometry. The P33 antibody (directed against amino acids 45–59 of Ad2 E3-19K) (gift from Dr. W. Wold, Saint Louis University School of Medicine, St. Louis, MO) was used in immunoblotting.

Cloning and Expression—Viral DNA was isolated from Ad37 (strain GW; a gift from J. Chodosh, Harvard Medical School, Boston) by digestion with proteinase K (100 μg/ml) (Invitrogen) at 37 °C for 1 h in 10 mM Tris, 1 mM EDTA, 0.6% SDS (pH 8.0) followed by phenol/chloroform extraction and ethanol precipitation. The cDNA encoding the signal peptide and ER lumenal domain (residues 1–95) of Ad37 E3-19K (referred to as Ad37 E3-19K) with a C-terminal His_6 sequence was generated by PCR using the isolated DNA of Ad37 as a template and the primers 5′-ACTGGATCCATGCTGGGTAAGACATTG-TGG-3′ (forward) and 5′-CCGGAATTCTCAATGGTGATG-GTGATGATGCTTGGTAGGGGGCCACAAGC-3′ (reverse). Similar strategies were used to clone Ad7 (residues 1–109), Ad35 (residues 1–109), Ad5 (residues 1–101), and Ad4 (residues 1–108) E3-19K proteins (the viral DNA of Ad7, Ad35, Ad5, and Ad4 were gifts of Drs. E. F. Pedersen (Cornell University Medical College, New York), M. Horwitz (deceased), and W. Wold). Ad2 E3-19K (residues 1–100) was generated as described previously (30). The cDNA encoding Ad2 E3-19K [K91E] (residues 1–100) was generated by the QuikChange site-directed mutational approach (Stratagene) using the Ad2 E3-19K/pFastBac plasmid as template. Recombinant, soluble E3-19K proteins were expressed using the Bac-to-Bac baculovirus expression system (Invitrogen) and purified as described previously (30).

Expression plasmids for the ER lumenal domains of HLA-A*0301, -A*1101, -A*3101, -A*3301, -Aw*6801, -B*0702, -B*0801, -Cw*0304, and -Cw*0401 heavy chains have been described previously (31). The cDNAs encoding the ER lumenal domains of HLA-A*1101[G56R], HLA-A*1101[E177K], and HLA-A*1101[G56R,E177K] heavy chains were generated by PCR using the QuikChange site-directed approach and the plasmids of HLA-A*1101 heavy chain as template (34). Plasmids harboring the correct DNA sequence were transformed into competent BL21(DE3)pLysS cells. Recombinant class I heavy chains and β_2-microglobulin (β_2m) were expressed as inclusion bodies in BL21(DE3)pLysS cells. Inclusion bodies were washed and solubilized in urea as described previously (35).

The cDNA of full-length HLA-A*1101[E177K] heavy chain was generated by the QuikChange approach using the plasmid pCR2.1-TOPO/HLA-A*1101 (a gift from Dr. P. Parham, Stanford University School of Medicine, Stanford, CA) as template, followed by insertion into the HindIII and XbaI restriction sites of the pcDNA3.1 vector (Invitrogen). The plasmid was linearized with BglII followed by transfection into C1R cells by electroporation as described previously (31). Stable transfectants expressing HLA-A*1101[E177K] were isolated by selection in 600 μg/ml G418 for 2–3 weeks. The cell-surface expression of HLA-A*1101[E177K] was determined by flow cytometry (see below).

The P631 plasmid was used for expression of full-length Ad2 E3-19K as described previously (36). The cDNA of full-length Ad2 E3-19K[K91E] was generated by the QuikChange approach using the P631 plasmid as template. The Ad2 E3-19K and Ad2 E3-19K[K91E] plasmids were then linearized with PvuI and each transfected into both A11/C1R and A31/C1R cells by electroporation to generate the following four co-transfectants: Ad2 E3-19K/A11/C1R, Ad2 E3-19K[K91E]/A11/C1R, Ad2 E3-19K/A31/C1R, and Ad2 E3-19K[K91E]/A31/C1R. The co-transfectants were cultured in RPMI 1640 medium supplemented with 10% FBS for 48 h followed by plating into 24-well plates. The selection of transfectants was initiated with 200 μg/ml Zeocin (Invitrogen) and 200 μg/ml hygromycin B for Ad2 E3-19K/A11/C1R and Ad2 E3-19K[K91E]/A11/C1R co-transfectants and with 200 μg/ml Zeocin and 300 μg/ml G418 for Ad2 E3-19K/A31/C1R and Ad2 E3-19K[K91E]/A31/C1R co-transfectants. After 2–3 weeks of selection, drug-resistant co-transfectants, which proliferated in many wells, were expanded and maintained individually in 100 μg/ml Zeocin and 200 μg/ml hygromycin B for Ad2 E3-19K/A11/C1R and Ad2

E3-19K[K91E]/A11/C1R co-transfectants and in 100 μg/ml Zeocin and 300 μg/ml G418 for Ad2 E3-19K/A31/C1R and Ad2 E3-19K[K91E]/A31/C1R co-transfectants. The expression levels of Ad2 E3-19K and Ad2 E3-19K[K91E] proteins in the co-transfectants were determined to be comparable by immunoblotting with the P33 antibody. Levels of cell-surface expression of HLA-A*1101 and -A*3101 were determined by flow cytometry (see below).

Viruses and Infection—Ad2 and H2dl801 (H2dl801 has a deletion in the gene encoding Ad2 E3-19K (37)) (a gift from Dr. W. Wold) were grown in HeLa S3 cells as described previously (31). Viruses were purified using the Adeno-X virus purification kit (Clontech) as described previously (31). A11/C1R and A11[E177K]/C1R cells (2.5×10^6 cells) were infected with Ad2 and H2dl801, respectively, at an estimated multiplicity of infection in the range of 60–100 in serum-free RPMI 1640 medium. After 1 h, 4 ml of RPMI 1640 medium containing 10% FBS was added to the cells. Mock infections (infection with serum-free RPMI 1640 medium) were carried out in an identical manner. Mock-, Ad2-, and H2dl801-infected transfectants were harvested at 48 h post-infection. Levels of cell-surface expression of HLA-A*1101 and HLA-A*1101[E177K] were determined by flow cytometry (see below).

Flow Cytometry—A11/C1R and A11[E177K]/C1R transfectants and Ad2 E3-19K/A11/C1R, Ad2 E3-19K[K91E]/A11/C1R, Ad2 E3-19K/A31/C1R, and Ad2 E3-19K[K91E]/A31/C1R co-transfectants were characterized by flow cytometry using an LSR instrument (BD Biosciences). All cells were washed twice with PBS containing 1% BSA and 0.1% NaN_3. The A11[E177K]/C1R transfectant was incubated at 4 °C using the mAb W6/32 for 45 min and the FITC-conjugated IgG for 45 min followed by sorting on a MoFlo high speed cell sorter (BD Biosciences) to pool the fraction of cells expressing the highest levels of HLA-A*1101[E177K]. Mock-, Ad2-, and H2dl801-infected A11/C1R and A11[E177K]/C1R transfectants were incubated with anti-HLA-A11 and the FITC-conjugated IgG, followed by fixing in 1% paraformaldehyde in the dark for 10 min. Ad2 E3-19K/A11/C1R and Ad2 E3-19K[K91E]/A11/C1R co-transfectants were incubated with anti-HLA-A11 and the FITC-conjugated IgG; Ad2 E3-19K/A31/C1R and Ad2 E3-19K[K91E]/A31/C1R co-transfectants were incubated with anti-HLA-A31 and the FITC-conjugated IgM. All cells were analyzed for MHC class I cell-surface expression by gating to exclude dead cells. Data analysis was performed using the Summit version 4.3 software (Beckman Coulter).

In Vitro Reconstitution of MHC Class I Molecules—Recombinant, soluble MHC class I molecules were assembled from the inclusion bodies of class I heavy chains and β_2m (or biotinylated β_2m) in the presence of synthetic peptides in an oxidative refolding buffer (35). Refolded β_2m was biotinylated as described previously (31). The MHC I-restricted peptides used for refolding have been described previously (31). Proteins were purified on a Superdex 200 HR 10/30 column in 20 mM Tris and 150 mM NaCl (pH 7.5).

Native Gel Band Shift Assay—E3-19K proteins (14 μg) were incubated with MHC class I molecules (20 μg) (2:1 molar ratio) on ice in 20 mM Tris and 150 mM NaCl (pH 7.5) for 30 min. The incubation mixtures were analyzed by native PAGE (10%) at 4 °C in 25 mM Tris and 200 mM glycine (pH 8.3). Proteins were visualized with Coomassie Blue R-250.

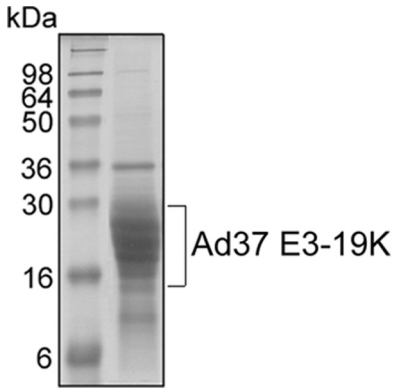

FIGURE 1. **Characterization of Ad37 E3-19K of subgroup D.** SDS-PAGE (15%) analysis of Ad37 E3-19K, with five potential *N*-linked glycans, from expression in High Five cells and after purification by gel filtration chromatography.

Surface Plasmon Resonance—Quantitative analyses of interaction in E3-19K/MHC I pairs were performed using SPR at 20 °C on a Biacore T100 instrument as described previously (31). Biotinylated MHC class I molecules were immobilized on a streptavidin-coated sensor chip (Series S Sensor chip SA, certified) at a density of ~750–800 resonance units using a stock solution (~30 nM) in HBS-EP (10 mM Hepes, 150 mM NaCl, 3 mM EDTA, and 0.05% Surfactant P-20 (pH 7.4)) at a flow rate of 60 μl/min. Uncoupled streptavidin sites were blocked with biotin (30 μl/min for 1 min). Solutions of E3-19K proteins (2.5 nM to 10 μM) were injected over the sample, and control flow cells (60 μl/min for 4 min) and binding responses (with control responses automatically subtracted) were recorded. Binding surfaces were regenerated with HBS-EP. Equilibrium dissociation constants were determined by plotting binding responses at steady state *versus* E3-19K concentrations based on a 1:1 Langmuir binding model using the Biacore T100 evaluation software (version 2.0.1, Biacore).

RESULTS

Expression and Characterization of E3-19K Proteins of Different Serotypes and Subgroups—We generated baculovirus systems for expression of soluble Ad7 (residues 1–109; subgroup B), Ad35 (residues 1–109; subgroup B), Ad5 (residues 1–101; subgroup C), Ad37 (residues 1–95; subgroup D), and Ad4 (residues 1–108; subgroup E) E3-19K proteins. Proteins were expressed in High Five insect cells at levels ranging from 0.2 to 3 mg of purified protein/liter of cell culture. The proteins migrated as closely spaced bands on SDS-polyacrylamide gel (*e.g.* see Fig. 1 for Ad37 E3-19K) because of *N*-glycosylation as demonstrated previously for Ad2 E3-19K (30). There are four cysteine residues that are absolutely conserved in the ER lumenal domain of all E3-19K proteins (38). These cysteine residues are paired, for example, as Cys^{11}/Cys^{28} and Cys^{22}/Cys^{83} in Ad2 E3-19K of subgroup C (38). Interestingly, with the exception of E3-19K proteins of subgroup C, all other E3-19K proteins have two additional conserved cysteine residues in their ER lumenal domains. We showed previously for Ad7 and Ad37 E3-19K pro-

teins (subgroups B and D, respectively) that these two Cys residues form a disulfide bond (39).

Qualitative and Quantitative Analysis of Interaction between E3-19K Proteins of Different Serotypes and Subgroups and MHC Class I Molecules—Interaction between E3-19K proteins of subgroups B (Ad7 and Ad35), C (Ad5), D (Ad37), and E (Ad4) and HLA-A (A*0301, A*1101, A*3101, A*3301, and Aw*6801), -B (B*0702 and B*0801), and -C (Cw*0304 and Cw*0401) molecules was monitored by a native gel band shift assay and SPR (Fig. 2 and Table 1, respectively). Results show that Ad37 E3-19K interacts with HLA-A molecules (Fig. 2*A*) as evidenced by new bands on the native gel that migrate at different positions from those of uncomplexed Ad37 E3-19K and HLA-A molecules. A quantitative analysis of interaction in Ad37 E3-19K/HLA-A complexes by SPR yielded equilibrium dissociation constants (K_d) of ~240 nM (Table 1). Interaction between E3-19K proteins of subgroups B, C, and E and the same HLA-A molecules was also determined by SPR (Table 1). The K_d values clearly indicate that these E3-19K proteins display allele-specific interaction with HLA-A molecules, a binding property that was less apparent for Ad37 E3-19K (at least with this particular set of HLA-A molecules). Interestingly, this allele specificity is remarkably similar for different serotypes of subgroup B (compare Ad7 with Ad35 E3-19K) as well as subgroup C (compare Ad2 with Ad5 E3-19K). Moreover, results from SPR show that, overall, Ad37 E3-19K of subgroup D exhibits the weakest binding affinities (highest K_d values) for HLA-A molecules, and Ad4 E3-19K of subgroup E displays the strongest binding affinities.

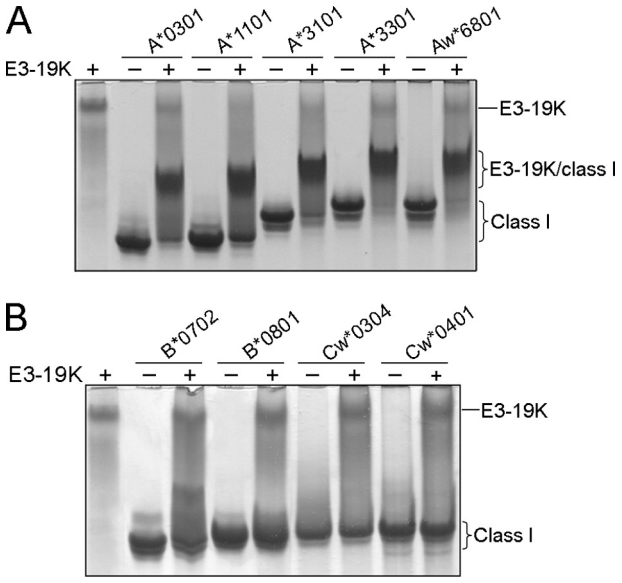

FIGURE 2. **Analysis of interaction between Ad37 E3-19K of subgroup D and HLA-A, -B, and -C molecules.** Samples of E3-19K (14 μg) were incubated with HLA-A molecules (20 μg) (*A*) and HLA-B and -C molecules (20 μg) (*B*) (2:1 molar ratio) on ice in 20 mM Tris, 150 mM NaCl (pH 7.5) for 30 min. After the addition of native gel loading buffer, the incubation mixtures were immediately loaded onto the native gel (10%) and run at 4 °C in 25 mM Tris, 200 mM glycine (pH 8.3).

The characterization of Ad37 E3-19K was extended to include interaction with HLA-B and -C molecules. Results from native gel (Fig. 2*B*) revealed that interaction between Ad37 E3-19K and HLA-B*0702 led to a protein smear with a very faint band at the expected position of a complex. In contrast, no new band could be seen on the gel for the mixture of Ad37 E3-19K and HLA-B*0801, although a weak smear of the HLA-B*0801 band could be observed. These results are consistent with Ad37 E3-19K interacting, at best, very weakly with HLA-B molecules causing complexes to dissociate during electrophoresis. Analysis of interaction with HLA-C molecules failed to produce new bands on the gel (Fig. 2*B*). Instead, intense and focused bands corresponding to uncomplexed Ad37 E3-19K and HLA-C molecules were observed, which is consistent with a lack of complex formation. Finally, interaction between Ad37 E3-19K and HLA-B molecules could not be determined reliably by SPR because of weak binding responses, and no interaction could be detected with HLA-Cw*0304 (Table 1). Taken together, these results show that Ad37 E3-19K manifests locus-specific interaction with MHC class I molecules, *i.e.* higher avidity with HLA-A relative to -B molecules and no interaction with HLA-C molecules. An SPR analysis of interaction between E3-19K proteins of subgroups B, C, and E and the same HLA-B and -C molecules (Table 1) revealed allele-specific interaction with HLA-B molecules and MHC I locus-specific interaction, as observed for Ad37 E3-19K.

Overall, results from native gel and SPR showed that E3-19K proteins of subgroups B–E exhibit allele-specific interaction (this was less apparent for Ad37 E3-19K of sub-

TABLE 1

Summary of equilibrium dissociation constants

Values were determined in duplicate by surface plasmon resonance at 20 °C (±S.D.).

	K_d (nM)						
	Subgroup B		Subgroup C		Subgroup D	Subgroup E	
Immobilized	Ad7	Ad35	Ad2[a]	Ad5	Ad37	Ad4	Ad2 E3-19K [K91E]
A*0301	43.3 ± 4.1	40.3 ± 0.2	14.9 ± 4.7	47.5 ± 1.6	260.3 ± 9	7.1 ± 0.3	
A*1101	48.7 ± 3.1	33.1 ± 0.9	15.5 ± 2.8	54.6 ± 3.3	242 ± 11.2	3.3 ± 0.2	637 ± 10.2
A*3101	117 ± 5.3	70.8 ± 0.8	255 ± 21	400 ± 4.1	263.2 ± 10	16.9 ± 0.1	2579 ± 100
A*3301	235 ± 7	225.4 ± 1.8	18.3 ± 3	55.8 ± 1.6	206.5 ± 8	16 ± 0.5	
Aw*6801	40.1 ± 0.5	35.4 ± 0.9	17.3 ± 1.7	67.7 ± 8.8	253 ± 9.3	8.3 ± 0.4	
B*0702	141 ± 4	198.2 ± 3.6	41.6	426 ± 10.4	ND[b]	ND	
B*0801	292.6 ± 7.4	85.3 ± 4.5	39.7 ± 4.3	102.3 ± 5	ND	290.7 ± 14	
Cw*0304	NB[c]		NB	NB	NB	NB	
A*1101[E177K]	136.9 ± 1.0	33.9 ± 4.6	2220 ± 105	3046 ± 191	ND	ND	
A*1101[G56R]	462 ± 9.2						
A*1101[G56R,E177K]	733 ± 18						

[a] K_d values were taken from Ref. 31 except for HLA-A*1101[E177K].
[b] ND means the K_d value could not be determined reliably.
[c] NB means no binding was detected.

group D) and MHC I locus specificity (higher avidity with HLA-A relative to -B molecules and no interaction with HLA-C molecules).

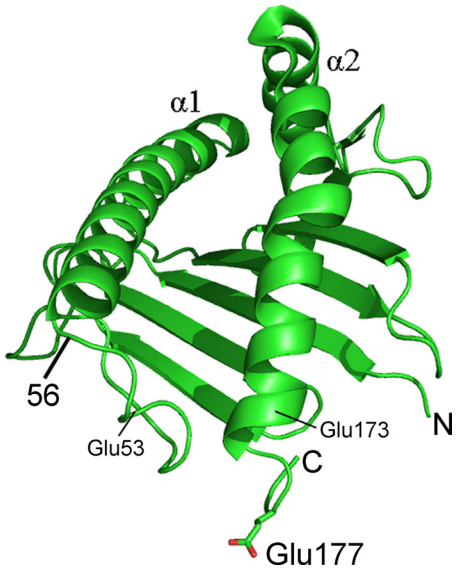

FIGURE 3. **Location of residues 56 and 177 in the peptide-binding groove of HLA-A*1101.** A close-up view along the groove of HLA-A*1101 (PDB code 1q94) showing residue 56 (Gly^{56} in HLA-A*1101 and solvent-exposed Arg^{56} in HLA-A*3101) at the N-terminal end of the α1-helix and conserved solvent-exposed residue Glu^{177} at the C-terminal end of the α2-helix. The conserved solvent-exposed residues Glu^{53} and Glu^{173} are also labeled. These residues represent potential interaction sites with conserved residues in E3-19K proteins. The backbone-to-backbone distance between residues 56 and 177 is 19.8 Å. The bound peptide is omitted in the groove and only Cα atoms are shown (except for the side chain of Glu^{177}). The N and C termini are indicated.

MHC Residue 177 Modulates Differentially the Immunomodulatory Function of E3-19K Proteins of Different Serotypes and Subgroups—Early studies have identified putative E3-19K-binding sites at both the N terminus of the α1-helix and the C terminus of the α2-helix (23, 24). Consistent with this, we showed previously that MHC residue 56, located at the N-terminal end of the α1-helix (Fig. 3), critically influences the immunomodulatory function of Ad2 E3-19K toward HLA-A molecules (31). Here, we sought to examine whether MHC residue 177 located at the C-terminal end of the α2-helix (Fig. 3) also plays a role in modulating interaction with E3-19K. Importantly, MHC 177 is a conserved and solvent-exposed Glu residue that occupies a position structurally equivalent to that of MHC 56, *i.e.* the end of an α-helical segment. These arguments make the negatively charged Glu^{177} a potential "hot spot" for E3-19K interaction on MHC class I molecules.

To assess the role of MHC residue 177, we introduced a Glu^{177} to Lys^{177} mutation in HLA-A*1101 heavy chain and monitored interaction first with Ad2 E3-19K (subgroup C) by native gel (Fig. 4*A*). Results clearly show that the E177K mutation in HLA-A*1101 abolished interaction with Ad2 E3-19K, relative to interaction with HLA-A*1101, as evidenced by the lack of a complex band and the presence of a strong band corresponding to uncomplexed HLA-A*1101[E177K]. We extended this analysis to include Ad7 and Ad35 (subgroup B), Ad5 (subgroup C), Ad37 (subgroup D), and Ad4 (subgroup E) E3-19K proteins (Fig. 4*A*). Results show that Ad5, Ad37, and Ad4 E3-19K proteins are also affected, most likely to a different extent, by the E177K mutation in HLA-A*1101 as indicated by

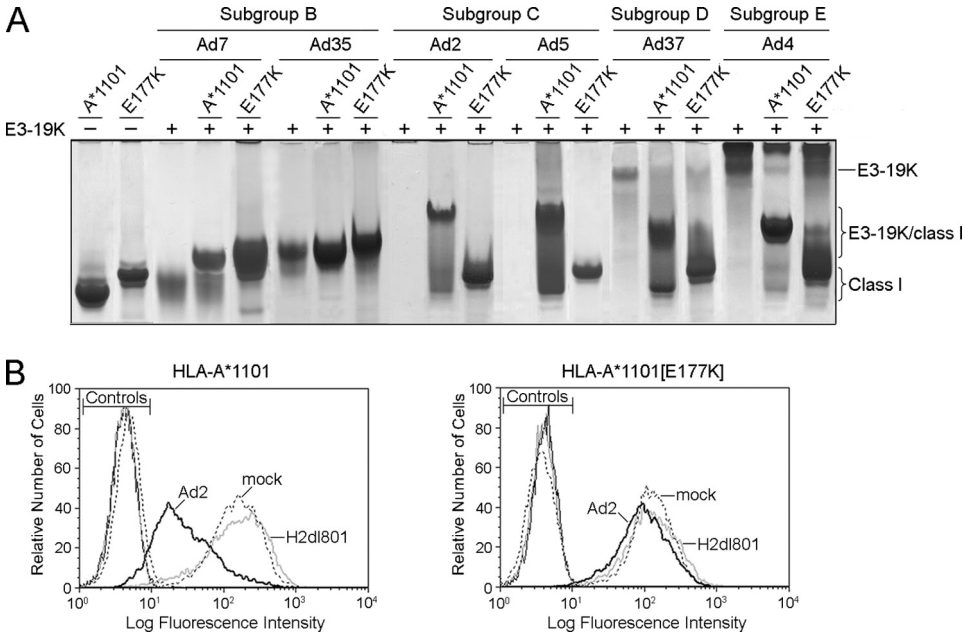

FIGURE 4. **MHC residue Glu^{177} modulates the MHC I binding function of E3-19K proteins of different serotypes and subgroups.** *A,* samples of Ad7 and Ad35 (subgroup B), Ad2 and Ad5 (subgroup C), Ad37 (subgroup D), and Ad4 (subgroup E) E3-19K proteins (14 μg) were incubated with HLA-A*1101 and HLA-A*1101[E177K] (20 μg) (2:1 molar ratio) as described in Fig. 2. The mixtures were loaded into the native gel (10%) that was run as described in Fig. 2. Note that the pI values of Ad2 and Ad5 E3-19K are 8.85 and 8.33, respectively; when pI values of proteins are above (or at) the pH of the running buffer (pH 8.3), they do not penetrate into the native gel (see Ref. 30 for a native gel of Ad2 E3-19K). *B,* expression of HLA-A*1101 (*left panel*) and HLA-A*1101[E177K] (*right panel*) on the surface of C1R cells was determined by flow cytometry at 48 h post-infection with Ad2 (*black lines*) using anti-HLA-A11 mAb. The expression of HLA-A*1101 and -A*1101[E177K] on the surface of mock- (*dotted black lines*) and H2dl801 (*gray lines*)-infected cells, determined under identical conditions, is shown in each panel. Controls were mock- (infection with RPMI 1640; *dotted black lines*), Ad2- (*black lines*), and H2dl801 (*gray lines*)-infected cells incubated with FITC-conjugated IgG alone. The mean logarithm fluorescence intensity of HLA-A*1101 and HLA-A*1101[E177K] expression on Ad2- and H2dl801-infected cells was normalized relative to that on mock-infected cells (which was set to 100%). *Histograms* are representative examples of three independent experiments.

the absence of strong bands at the expected positions of E3-19K/HLA-A*1101[E177K] complexes and of intense bands corresponding to uncomplexed HLA-A*1101[E177K]. In marked contrast, however, results clearly show that Ad7 and Ad35 E3-19K proteins of subgroup B associate with HLA-A*1101[E177K] as evidenced by the presence of new bands corresponding to E3-19K/HLA-A*1101[E177K] complexes and of very faint bands at the position of uncomplexed HLA-A*1101[E177K]. Taken together, results from the native gel show that the ability of E3-19K proteins of subgroups C–E to associate with HLA-A*1101 is affected by a mutation in MHC residue 177 in HLA-A*1101. In contrast, E3-19K proteins of subgroup B are evidently less affected by this particular mutation.

An analysis of interaction in E3-19K/HLA-A*1101[E177K] pairs was carried out by SPR to firmly establish the role of MHC residue 177 in the MHC I binding function of E3-19K (Table 1). Results show that the K_d values are considerably higher (lower affinity) for Ad2 and Ad5 E3-19K proteins interacting with HLA-A*1101[E177K] (2220 ± 105 and 3046 ± 191 nM, respectively) relative to HLA-A*1101 (15.5 ± 2.8 and 54.6 ± 3.3 nM, respectively). The K_d values could not be determined reliably for Ad37 and Ad4 E3-19K proteins suggesting very weak interaction with HLA-A*1101[E177K]. In striking contrast, the K_d value of Ad7 E3-19K is moderately higher for HLA-A*1101[E177K] (136.9 ± 1.0 nM) relative to HLA-A*1101 (48.7 ± 3.1 nM), whereas that of Ad35 E3-19K is essentially unchanged (Table 1). Thus, overall, results from SPR extend those from native gel and provide convincing evidence that MHC residue 177 in HLA-A*1101 is critical for interaction with E3-19K proteins and that the extent of its modulating effect differs with serotypes and subgroups.

To show that the effect of MHC residue 177 on interaction with Ad2 E3-19K has functional consequences in cells, Ad2-infected C1R cells stably expressing HLA-A*1101[E177K] were characterized by flow cytometry (Fig. 4*B*). The cell-surface expression of HLA-A*1101[E177K] on infected C1R cells, relative to mock-infected cells, was determined to be 83.6%. This is significantly higher than the cell-surface expression of HLA-A*1101, which was determined to be 25.2% under identical conditions. This effect on MHC I expression was specific to E3-19K as infection of C1R cells with H2dl801 virus lacking the gene encoding Ad2 E3-19K (37) had essentially no effect on cell-surface expression of HLA-A*1101[E177K] and HLA-A*1101 (Fig. 4*B*). Taken together, the significantly weaker affinity of Ad2 E3-19K for HLA-A*1101[E177K] (Table 1), relative to HLA-A*1101, allowed the mutant to escape retention in the ER of infected C1R cells and, consequently, be expressed at significantly higher levels on the cell surface.

Overall, results from native gel, SPR, and flow cytometry unambiguously show that MHC residue 177 in HLA-A*1101 critically influences the immunomodulatory function of E3-19K proteins in a way that varies according to serotypes and subgroups. Thus, in addition to MHC 56, we have identified MHC 177 as another important E3-19K-binding site on MHC class I molecules.

MHC Residues 56 and 177, Insights into the E3-19K-Binding Mode—A close examination of our *in vitro* binding data (Table 1) shows that E3-19K proteins of subgroups B, D, and E, but not those of subgroup C, display rather similar binding affinities for HLA-A*3101 relative to other HLA-A molecules. It is the noticeably weaker affinity of Ad2 E3-19K of subgroup C for HLA-A*3101 (Table 1), together with an analysis of MHC I polymorphism, that allowed us previously to identify a critical role for MHC residue 56 on the immunomodulatory function of Ad2 E3-19K (31). Our new SPR results extend this earlier finding and show that MHC 56, in a way similar to MHC 177, modulates the MHC I binding function of E3-19K proteins in a manner that varies with serotypes and subgroups. Because our results on MHC residues 56 and 177 were obtained using different E3-19K/MHC I pairs (E3-19K/HLA-A*3101 for MHC 56 and E3-19K/HLA-A*1101 for MHC 177), we sought here to carry out a side-by-side comparison of mutations at MHC 56 and 177 in the Ad7 E3-19K/HLA-A*1101 pair to further characterize the binding mode of E3-19K. For this, we monitored and compared interaction of Ad7 E3-19K with HLA-A*1101[G56R], HLA-A*1101[E177K] (discussed above), and the double mutant HLA-A*1101[G56R,E177K] using SPR (Table 1). The K_d values indicate that mutations at positions 56 (462 ± 9.2 nM) and 177 (136.9 ± 1.0 nM) each weakened interaction with Ad7 E3-19K relative to HLA-A*1101 (48.7 ± 3.1 nM). Interestingly, the mutation at residue 56 had a noticeably more suppressing effect on interaction with E3-19K than the mutation at residue 177. Finally, the K_d value for Ad7 E3-19K association with the double mutant HLA-A*1101[G56R,E177K] is 733 ± 18 nM. This value is higher than the K_d values of either of the single mutants and thus most likely reflects a combination of their individual suppressing effects. Taken together, these studies provide evidence that the Ad7 E3-19K/HLA-A*1101 interface includes interaction with both MHC residues 56 and 177 and that MHC 56 likely represents a more dominant contact site in the complex.

Lys^{91} in Ad2 E3-19K Targets the C Terminus of the α2-Helix on MHC Class I Molecules—To date, we have a rather weak understanding of how E3-19K uses its variable and conserved regions to associate with MHC class I molecules. This knowledge is important as it undoubtedly can help understand the molecular basis of differential interaction in E3-19K/MHC I pairs. In a very recent study (36), we showed that residues 89–93 (^{89}MSKQY^{93}) in the conserved region of Ad2 E3-19K are essential for its immunomodulatory function. Here, to gain insights into where this critical stretch of residues from the conserved region preferentially binds on MHC class I molecules, *i.e.* at the N terminus of the α1-helix or the C terminus of the α2-helix (Fig. 3), we introduced a Lys^{91} to Glu^{91} mutation in Ad2 E3-19K and monitored interaction with HLA-A*1101 and HLA-A*3101 using a native gel band shift assay. First, note that Lys^{91} is conserved (or substituted by Arg residue) in all E3-19K proteins (numbering of the equivalent Lys or Arg varies with serotypes) thus suggesting an important functional role for this residue. Second, as shown in Fig. 3, the N terminus of the α1-helix in HLA-A*1101 has Gly^{56}, whereas that in HLA-A*3101 carries Arg^{56}, and the C terminus of the α2-helix in both of these alleles carries Glu^{177}. Finally, we showed previ-

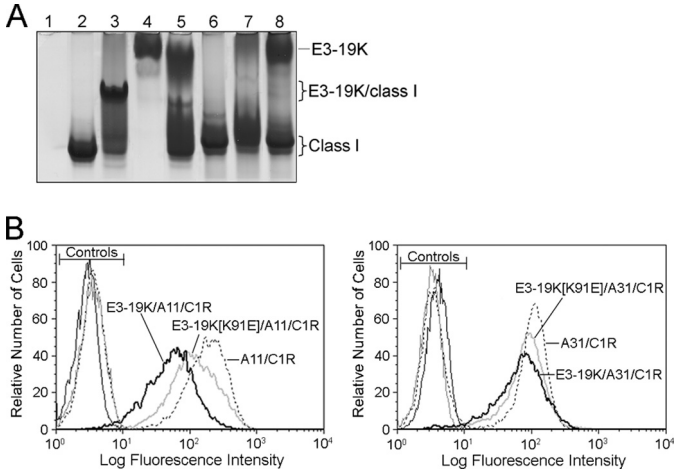

FIGURE 5. **Lys[91] in the conserved region of Ad2 E3-19K binds to the site of Glu[177] on MHC class I molecules.** *A,* samples of Ad2 E3-19K (*lane 1*) and Ad2 E3-19K[K91E] (*lane 4*) (14 μg) were each incubated with HLA-A*1101 (*lane 2*) and HLA-A*3101 (*lane 6*) (20 μg) (2:1 molar ratio) as described in Fig. 2. The incubation mixtures (*lanes 3* and *5*, respectively, for HLA-A*1101 and *lanes 7* and *8*, respectively, for HLA-A*3101) were loaded into the native gel (10%) that was run as described in Fig. 2. *B,* expression of HLA-A*1101 (*left panel*) and HLA-A*3101 (*right panel*) on C1R co-transfectants was determined by flow cytometry after staining with either anti-HLA-A11 or anti-HLA-A31 mAbs. *Black lines* represent Ad2 E3-19K/A11/C1R and Ad2 E3-19K/A31/C1R co-transfectants; *gray lines* represent Ad2 E3-19K[K91E]/A11/C1R and Ad2 E3-19K[K91E]/A31/C1R co-transfectants. The expression of HLA-A*1101 and -A*3101 on the surface of C1R cells (*dotted black lines*) is shown in each panel. Controls were HLA-A*1101 (*dotted black lines*), HLA-A*3101 (*dotted black lines*), and co-transfectants incubated with FITC-conjugated IgG (Ad2 E3-19K/A11/C1R, *black lines*; Ad2 E3-19K[K91E]/A11/C1R, *gray lines*) or FITC-conjugated IgM alone (Ad2 E3-19K/A31/C1R, *black lines*; Ad2 E3-19K[K91E]/A31/C1R, *gray lines*). At least three clones for each co-transfectant showing comparable expression levels of E3-19K or E3-19K[K91E] were analyzed. The mean logarithm fluorescence intensity of HLA-A*1101 and HLA-A*3101 expression on co-transfectants was normalized relative to that on A11/C1R and A31/C1R cells, respectively (which was set to 100%).

ously that Ad2 E3-19K binds strongly to HLA-A*1101 but considerably more weakly to HLA-A*3101 (see Table 1) (32). Taken together, an analysis of interaction between E3-19K[K91E] and HLA-A*1101 and HLA-A*3101 will likely allow us to distinguish just how E3-19K uses a critical stretch of residues from its conserved region to target MHC class I molecules, *i.e.* through interactions at the N terminus of the α1-helix or the C terminus of the α2-helix.

The incubation mixtures of Ad2 E3-19K (*lane 1* in Fig. 5*A*) and Ad2 E3-19K[K91E] (*lane 4*) with HLA-A*1101 (*lane 2*) clearly show that the K91E mutation in Ad2 E3-19K weakened interaction with HLA-A*1101 as evidenced in *lane 5* by the considerably fainter band at the expected position of a complex (compare *lane 3* for Ad2 E3-19K/HLA-A*1101 with *lane 5* for Ad2 E3-19K[K91E]/HLA-A*1101). A similar analysis revealed that the K91E mutation in Ad2 E3-19K also affected interaction with HLA-A*3101 (Fig. 5*A, lane 6*) as evidenced in *lane 8* by the lack of a protein smear at the expected position of a complex (compare *lane 7* for Ad2 E3-19K/HLA-A*3101 with *lane 8* for Ad2 E3-19K[K91E]/HLA-A*3101) and the presence of strong bands corresponding to uncomplexed Ad2 E3-19K[K91E] and HLA-A*3101. Taken together, results from native gel show that the K91E mutation in Ad2 E3-19K markedly suppressed interaction with both HLA-A*1101 and HLA-A*3101.

Our data from native gel were extended by a quantitative analysis of interaction in Ad2 E3-19K[K91E]/MHC I pairs using SPR (Table 1). The K_d values show that Ad2 E3-19K[K91E], in comparison to Ad2 E3-19K, interacts considerably more weakly with HLA-A*1101 and -A*3101 (Table 1), 637 $\pm$ 10.2 *versus* 15.5 $\pm$ 2.8 nM for HLA-A*1101 and 2579 $\pm$ 100 *versus* 255 $\pm$ 21 nM for HLA-A*3101. Taken together, a reasonable interpretation of native gel and SPR results is as follows. First, that Ad2 E3-19K[K91E] failed to interact with HLA-A*3101 (see Fig. 5*A, lane 8,* and Table 1) suggests that the negatively charged Glu[91] in Ad2 E3-19K[K91E] is unlikely to target the site of the positively charged Arg[56] at the N terminus of the α1-helix (Fig. 3) as this would have otherwise resulted in a favorable electrostatic interaction and promoted complex formation. Second, that Ad2 E3-19K[K91E] showed weakened interaction not only with HLA-A*3101 but also with HLA-A*1101 (see Fig. 5*A, lane 5,* and Table 1) can be accounted for on the basis of repulsive electrostatic interactions between the negatively charged residues Glu[91] in Ad2 E3-19K[K91E] and the negatively charged Glu[177] at the C terminus of the α2-helix of both HLA-A*3101 and HLA-A*1101 (Fig. 3). Our results are therefore more consistent with the conserved region of Ad2 E3-19K, in particular the stretch of residues near Lys[91], targeting the C-terminal end of the α2-helix (MHC residue 177) rather than the N-terminal end of the α1-helix on MHC class I molecules (see Fig. 3 and model under the "Discussion").

Finally, to validate our biochemical observations, we used a functional assay based on measurements of HLA-A*1101 and -A*3101 expression levels on the surface of C1R cells co-transfected with either Ad2 E3-19K or Ad2 E3-19K[K91E]. Results show that, relative to A11/C1R cells, expression levels of HLA-A*1101 (Fig. 5*B*) on Ad2 E3-19K/A11/C1R and Ad2 E3-19K[K91E]/A11/C1R co-transfectants were 35.1 and 75.2%, respectively. These results correlate with the differential affinities of Ad2 E3-19K and Ad2 E3-19K[K91E] for HLA-A*1101 (Table 1); the considerably more weakly bound Ad2 E3-19K[K91E]/HLA-A*1101 complex allowed HLA-A*1101 to be expressed on the surface of C1R cells at significantly higher levels. A similar analysis with HLA-A*3101 showed that this allele is, however, expressed at similarly high levels on the surface of both Ad2 E3-19K/A31/C1R and Ad2 E3-19K[K91E]/A31/C1R co-transfectants (Fig. 5*B*), 77.2 *versus* 83.2%, respectively. These results suggest that for intrinsically weak complexes such as the Ad2 E3-19K/HLA-A*3101 complex, effects that further weaken binding affinities do not necessarily translate into markedly higher levels of MHC I cell-surface expression.

Taken together, these biochemical and functional analyses have provided evidence that Lys[91] in the conserved region of Ad2 E3-19K is functionally important and that this residue most likely associates with MHC class I molecules through interactions at the C terminus of the α2-helix rather than the N terminus of the α1-helix.

DISCUSSION

A key finding from our characterization of interaction in E3-19K/MHC I pairs is that E3-19K proteins of subgroups B, C, and E display allele-specific interaction with HLA-A and -B molecules; this effect was less obvious for Ad37 E3-19K of subgroup D (at least with this particular set of HLA-A and -B mol-

ecules). In a previous study (31) (Table 1), we showed that Ad2 E3-19K displays allele-specific interaction with HLA-A molecules and, importantly, that this specificity correlates (in a negative way) with levels of MHC I expression on Ad2-infected C1R cells. This functional link is further supported here from our data on the differential association of Ad2 E3-19K with HLA-A*1101 relative to both HLA-A*1101[E177K] and Ad2 E3-19K[K91E] mutants. Thus, allele-specific interaction is a common property of E3-19K proteins, and binding affinities correlate (in a negative way) with levels of MHC I cell-surface expression on infected cells. As expected, our data also indicated that this correlation is less evident for E3-19K/MHC I pairs that have intrinsically weak affinities, *i.e.* intrinsically high levels of MHC I cell-surface expression.

Our results also indicate that the allele specificity of E3-19K proteins for HLA-A molecules is remarkably similar for serotypes of subgroup B as well as subgroup C. Furthermore, our results indicated that Ad37 E3-19K of subgroup D has the weakest binding affinities, although Ad4 E3-19K of subgroup E has the highest binding affinities for HLA-A molecules. Interestingly, it was reported previously that immunoprecipitates of MHC class I molecules from Ad-infected 293 cells co-precipitated Ad2 E3-19K (subgroup C) but not Ad19a E3-19K (subgroup D) (40). Because the amino acid sequence of Ad19a E3-19K is identical to that of Ad37 E3-19K, this result is consistent with our finding that Ad37 E3-19K binds very weakly to MHC class I molecules. From these studies, we infer that the different MHC I binding properties of E3-19K proteins are the manifestation of differences in key amino acids at the E3-19K/MHC I interface.

Our binding data also showed that E3-19K proteins of subgroups B, C, D, and E display the same locus-specific interaction with MHC class I molecules, *i.e.* stronger affinities with HLA-A compared with HLA-B molecules, and no interaction with HLA-C molecules. This ability of E3-19K proteins to distinguish between *MHC* gene products may represent a survival mechanism evolved by Ads to selectively manipulate host CTL and natural killer (NK) cell functions. Indeed, given that HLA-A and -B molecules present viral peptides specifically to receptors on CTLs and that HLA-C molecules present viral peptides specifically to inhibitory receptors on NK cells (41), the MHC I locus specificity of E3-19K proteins may predispose Ads to avoid clearance by both CTLs and NK cells. Other viral immunomodulatory proteins such as the Kaposi sarcoma-associated herpesvirus K5 protein (42) and Nef from HIV-1 (43) display the same MHC I locus specificity, a property that has been shown to protect virally infected cells from lysis by NK cells (42, 43). Note that this potential inhibitory mechanism of NK cells is distinct from that proposed recently by McSharry *et al.* (44) in which E3-19K sequesters MHC I chain-related proteins A and B molecules, *i.e.* the ligands of the activating NK receptor NKG2D.

From our binding and cell-based studies, we identified MHC residue 177 in HLA-A*1101 as a critical residue for the immunomodulatory function of E3-19K proteins. More specifically, we showed that the extent of MHC 177-modulating effects on E3-19K proteins varies with serotypes and subgroups, with serotypes of subgroup B being less sensitive to modulation than those of subgroups C–E. Studies of interaction between HLA-A*3101 and E3-19K proteins also allowed us to conclude that, in a manner similar to MHC 177, MHC 56 differentially modulates the MHC I binding function of E3-19K proteins. Importantly, a characterization of interaction between Ad7 E3-19K and the double mutant HLA-A*1101[G56R,E177K] showed that MHC residues 56 and 177 are both part of the Ad7 E3-19K/HLA-A*1101 interface, with MHC 56 being a more dominant contact site. Interestingly, the backbone-to-backbone distance between MHC residues 56 and 177 (see Fig. 3) is 19.8 Å, and assuming that E3-19K adopts an Ig-like structure (45), its longest dimension would be roughly 33 Å (approximated from the x-ray structures of Ig-like proteins such as β_2m, US2, and the α3-domain of MHC class I heavy chain). Thus, it is entirely reasonable to suggest that the E3-19K structure can span the distance of 19.8 Å. This analysis further supports our experimental findings that MHC residues 56 and 177 are both contacts sites in the Ad7 E3-19K/HLA-A*1101 complex.

On the basis of our data, we propose a model of interaction in E3-19K/MHC I pairs in which all E3-19K proteins establish evolutionally conserved interactions with MHC residues at both the N terminus of the α1-helix and the C terminus of the α2-helix of the peptide-binding groove. As suggested by our data, E3-19K proteins most likely use residues from its conserved region, such as the conserved Lys^{91}, to mediate interaction with conserved MHC residues, such as Glu^{177}, at the C-terminal end of the α2-helix. Note that there are at least two other conserved and negatively charged solvent-exposed MHC residues at the N-terminal end of the binding groove, namely Glu^{53} and Glu^{173} (see Fig. 3), that may also be important for interaction with conserved residues in E3-19K proteins. These evolutionally conserved interactions would provide a basal level of stabilizing energy to the E3-19K/MHC I association. In our model, we also suggest that these interactions are supplemented by other important contacts at both the N terminus of the α1-helix and the C terminus of the α2-helix of the groove that involves residues from the variable region of E3-19K. These contacts would contribute additional binding energy to the E3-19K/MHC I association, the extent of which can vary with serotypes and subgroups depending on the complementarity of the interacting surfaces. Consequently, and as supported by our data, to achieve optimal stabilizing interaction at the E3-19K/MHC I interface, either the N terminus of the α1-helix or the C terminus of the α2-helix will serve as a dominant binding region in different E3-19K/MHC I pairs. This view on the conserved and variable regions in the E3-19K/MHC I association accounts for why 1) E3-19K proteins of subgroup B or C, which have high levels of sequence homology in their variable regions, display similar allele specificity toward HLA-A molecules; and 2) E3-19K proteins of different subgroups, which show considerably lower levels of sequence homology in their variable regions, display distinctively different binding affinities (K_d values) for a given HLA-A molecule.

The critical role of MHC class I molecules in host antiviral immunity has put tremendous pressure on viruses to evolve escape mechanisms from immune surveillance. For Ads, this is achieved through the intriguing E3-19K protein that targets MHC class I molecules for retention in the ER. In this study, we

have provided new information on the MHC I binding properties of E3-19K proteins of different serotypes and subgroups. From this, a picture is emerging on how E3-19K, with a unique arrangement of variable and conserved domains, mediates interaction with its cellular target. This knowledge contributes to move forward our understanding at the molecular level of E3-19K function. Also, our results showing major differences in the strength of interaction in different E3-19K/MHC I pairs more firmly establish the notion that this association plays an important role in the pathogenesis of Ads. In a clinical setting, information on Ad serotypes and subgroups and HLA background of immunocompromised patients is potentially useful to identify patients who may be at higher risks of developing Ad diseases.

REFERENCES

1. Green, M., Mackey, J. K., Wold, W. S., and Rigden, P. (1979) *Virology* **93,** 481–492
2. Wadell, G. (1984) *Curr. Top. Microbiol. Immunol.* **110,** 191–220
3. Fox, J. P., Brandt, C. D., Wassermann, F. E., Hall, C. E., Spigland, I., Kogon, A., and Elveback, L. R. (1969) *Am. J. Epidemiol.* **89,** 25–50
4. Fox, J. P., Hall, C. E., and Cooney, M. K. (1977) *Am. J. Epidemiol.* **105,** 362–386
5. Hierholzer, J. C. (1992) *Clin. Microbiol. Rev.* **5,** 262–274
6. Flomenberg, P., Babbitt, J., Drobyski, W. R., Ash, R. C., Carrigan, D. R., Sedmak, G. V., McAuliffe, T., Camitta, B., Horowitz, M. M., Bunin, N., and Casper, J. T. (1994) *J. Infect. Dis.* **169,** 775–781
7. Zahradnik, J. M., Spencer, M. J., and Porter, D. D. (1980) *Am. J. Med.* **68,** 725–732
8. Krilov, L. R., Rubin, L. G., Frogel, M., Gloster, E., Ni, K., Kaplan, M., and Lipson, S. M. (1990) *Rev. Infect. Dis.* **12,** 303–307
9. Andersson, M., Pääbo, S., Nilsson, T., and Peterson, P. A. (1985) *Cell* **43,** 215–222
10. Andersson, M., McMichael, A., and Peterson, P. A. (1987) *J. Immunol.* **138,** 3960–3966
11. Burgert, H. G., and Kvist, S. (1985) *Cell* **41,** 987–997
12. Burgert, H. G., and Kvist, S. (1987) *EMBO J.* **6,** 2019–2026
13. Cox, J. H., Yewdell, J. W., Eisenlohr, L. C., Johnson, P. R., and Bennink, J. R. (1990) *Science* **247,** 715–718
14. Kvist, S., Ostberg, L., Persson, H., Philipson, L., and Peterson, P. A. (1978) *Proc. Natl. Acad. Sci. U.S.A.* **75,** 5674–5678
15. Burgert, H. G., Maryanski, J. L., and Kvist, S. (1987) *Proc. Natl. Acad. Sci. U.S.A.* **84,** 1356–1360
16. Flomenberg, P., Piaskowski, V., Truitt, R. L., and Casper, J. T. (1996) *J. Virol.* **70,** 6314–6322
17. Rawle, F. C., Tollefson, A. E., Wold, W. S., and Gooding, L. R. (1989) *J. Immunol.* **143,** 2031–2037
18. Tanaka, Y., and Tevethia, S. S. (1988) *Virology* **165,** 357–366
19. Ginsberg, H. S., Lundholm-Beauchamp, U., Horswood, R. L., Pernis, B., Wold, W. S., Chanock, R. M., and Prince, G. A. (1989) *Proc. Natl. Acad. Sci. U.S.A.* **86,** 3823–3827
20. Burgert, H. G., Ruzsics, Z., Obermeier, S., Hilgendorf, A., Windheim, M., and Elsing, A. (2002) in *Viral Proteins Counteracting Host Defenses* (Koszinowski, U. H., and Hengel, H., eds) pp. 273–318, Springer-Verlag, Berlin
21. Wold, W. S., and Gooding, L. R. (1989) *Mol. Biol. Med.* **6,** 433–452
22. Beier, D. C., Cox, J. H., Vining, D. R., Cresswell, P., and Engelhard, V. H. (1994) *J. Immunol.* **152,** 3862–3872
23. Feuerbach, D., Etteldorf, S., Ebenau-Jehle, C., Abastado, J. P., Madden, D., and Burgert, H. G. (1994) *J. Immunol.* **153,** 1626–1636
24. Flomenberg, P., Gutierrez, E., and Hogan, K. T. (1994) *Mol. Immunol.* **31,** 1277–1284
25. Gabathuler, R., Lévy, F., and Kvist, S. (1990) *J. Virol.* **64,** 3679–3685
26. Hermiston, T. W., Tripp, R. A., Sparer, T., Gooding, L. R., and Wold, W. S. (1993) *J. Virol.* **67,** 5289–5298
27. Cox, J. H., Bennink, J. R., and Yewdell, J. W. (1991) *J. Exp. Med.* **174,** 1629–1637
28. Pääbo, S., Bhat, B. M., Wold, W. S., and Peterson, P. A. (1987) *Cell* **50,** 311–317
29. Flomenberg, P., Szmulewicz, J., Gutierrez, E., and Lupatkin, H. (1992) *J. Virol.* **66,** 4778–4783
30. Liu, H., Stafford, W. F., and Bouvier, M. (2005) *J. Virol.* **79,** 13317–13325
31. Liu, H., Fu, J., and Bouvier, M. (2007) *J. Immunol.* **178,** 4567–4575
32. Severinsson, L., Martens, I., and Peterson, P. A. (1986) *J. Immunol.* **137,** 1003–1009
33. Hermiston, T. W., Hellwig, R., Hierholzer, J. C., and Wold, W. S. (1993) *Virology* **197,** 593–600
34. Li, L., Promadej, N., McNicholl, J. M., and Bouvier, M. (2002) *Acta Crystallogr. D Biol. Crystallogr.* **58**, 1195–1197
35. Garboczi, D. N., Hung, D. T., and Wiley, D. C. (1992) *Proc. Natl. Acad. Sci. U.S.A.* **89,** 3429–3433
36. Fu, J., and Bouvier, M. (2011) *Mol. Immunol.* **48,** 532–538
37. Challberg, S. S., and Ketner, G. (1981) *Virology* **114,** 196–209
38. Sester, M., and Burgert, H. G. (1994) *J. Virol.* **68,** 5423–5432
39. Fu, J., Lee, B. S., and Bouvier, M. (2009) in *Proceedings of the 2nd European Congress of Immunology, Berlin, September 13–16, 2009* (Schmidt, R. E., ed) pp. 123–126, Medimond, Berlin, Germany
40. Deryckere, F., and Burgert, H. G. (1996) *J. Virol.* **70,** 2832–2841
41. Yokoyama, W. M. (1998) *Curr. Opin. Immunol.* **10,** 298–305
42. Ishido, S., Wang, C., Lee, B. S., Cohen, G. B., and Jung, J. U. (2000) *J. Virol.* **74,** 5300–5309
43. Cohen, G. B., Gandhi, R. T., Davis, D. M., Mandelboim, O., Chen, B. K., Strominger, J. L., and Baltimore, D. (1999) *Immunity* **10,** 661–671
44. McSharry, B. P., Burgert, H. G., Owen, D. P., Stanton, R. J., Prod'homme, V., Sester, M., Koebernick, K., Groh, V., Spies, T., Cox, S., Little, A. M., Wang, E. C., Tomasec, P., and Wilkinson, G. W. (2008) *J. Virol.* **82,** 4585–4594
45. Chatterjee, D., and Maizel, J. V., Jr. (1984) *Proc. Natl. Acad. Sci. U.S.A.* **81,** 6039–6043